Intercalation of cations in crystalline anionic surfactants

Yutaka Abe,[a]*† Kazuaki Harata,[a] Masami Fujiwara[b] and Kazuo Ohbu[b]

[a] *National Institute of Bioscience and Human-Technology, 1-1 Higashi, Tsukuba, Ibaraki 305, Japan*
[b] *Material Science Research Center, Lion Corporation, 7-13-12 Hirai, Edogawa-ku, Tokyo 132, Japan*

Received (in Cambridge) 10th August 1998, Accepted 27th October 1998

Crystal structures of sodium, potassium and cesium salts of anionic surfactants, methyl 2-sulfoalkanoates, were analyzed by X-ray methods to characterize physico-chemical properties of the solid state in relation to counter ions. The crystal contains racemic molecules with the stereogenic β carbon atom. The crystals have a bilayer structure with the interdigitated alkyl chain of anions, while the cations and water molecules are intercalated between the layers. These crystals have different thermal stability indicated by the decrease in melting temperature in the order of potassium, cesium and sodium salts. The crystals of sodium, potassium and cesium salts contain two, one and one water molecules, respectively. The space group is *Pbca* for all of these crystals having the same type of crystal packing of anions regardless of the different cations. The crystal packing of the potassium salts is not significantly affected by the alkyl chain length, except for the difference in the *c* dimension. The energetic difference of the crystal structures was analyzed by molecular mechanics calculations using X-ray coordinates. The thermal stability of the crystal is related to the crystal structure, especially to the packing of cations and sulfonato groups between the layers. The potassium ion contributes more to the thermal stabilization of the crystal than the sodium and cesium ions because of more effective contact with the sulfonato groups by less coordination with the water molecule and by acquired electrostatic potential. The close packing of ionic layers observed in the crystals of potassium salts causes dense packing of the alkyl chains which stabilizes the crystal packing.

Introduction

We report the X-ray structures of anionic surfactants to investigate relations between the crystal structures and physico-chemical properties. The crystalline state of surfactants has been of interest from the viewpoint of supramolecular chemistry.[1] Crystals of surfactants have a bilayer structure similar to that of a cell membrane organized with phospholipid.[2,3] Some surfactants crystallize as inclusion compounds with small organic molecules.[1] Counter ions are located in the crystals of ionic surfactants between anionic layers forming a structure like clathrate compounds. The crystals of surfactants are also of interest from the classical viewpoint. Kraft points, the triple point of the aqueous surfactant solution with a solid, monomer and micelle state, are important physico-chemical parameters reflecting the solubility of surfactants in an aqueous system and have been studied since the 1890s.[4] Surfactants are mostly used in aqueous systems, but the precipitation and insolubility of surfactants in solution decrease surface activity. The thermal stability of the solid state of anionic surfactants depends on counter ions[5] which affect the Kraft point, for example, 7 and 34 °C for sodium and potassium dodecyl sulfate, respectively.[6,7] The molecular arrangement in the solid state differs between those salts, but the details of the mechanism of dissolution have not been clarified. Methyl 2-sulfoalkanoate potassium salts (MSA·K) have higher Kraft points than those of the sodium salts.[5] The critical micelle concentration of the surfactant is slightly different among cations with the same charge.[8] Therefore, these surfactants have different aqueous solubility depending on the cations. This suggests that the solid state of the surfactant recognizes the types of cations.

The solid state of the surfactants is mostly crystalline.[9,10] Crystal structures are related to the physico-chemical properties of the solid state and provide important information to elucidate the properties.[11] The crystal structures of amphiphiles, phospholipids,[3] glycolipids[11–17] and aliphatic acids[18,19] have been reported. Those structures of amphiphiles have been discussed in relation to the thermal stability of the crystalline state.[11] However only a few crystal structures of surfactants have been rarely reported, especially for anionic surfactants, because of the difficulty in the preparation of single crystals for X-ray measurement. Only the crystal structures of sodium dodecyl sulfate 1/8 hydrate[2] and hemi-hydrate have been reported, but no systematic analyses of the crystal structures of anionic surfactants have been performed to compare different types of cations.[20]

We have been investigating the physico-chemical properties of MSA salts.[21–25] MSA salts derived from aliphatic acids or methyl alkanoates have been used as anionic surfactants in commodity detergents. The X-ray powder patterns and thermal analysis of crystalline sodium MSA salts which have different hydrate numbers have been reported as well as those of sodium dodecyl sulfate (SDS).[9,24]

We have obtained single crystals of MSA salts with different types of cations. Previously we reported the structures relating to the physico-chemical properties of glycolipids. The preliminary X-ray structure of MSA·Na has been reported,[25] and full structures for a series of cations will be shown in this report. This is the first report which describes the details of the structures and thermal stability of crystalline MSA salts and discusses the effect of cations on the crystal packing of the anionic surfactants.

Experimental

Materials listed in Table 1 were produced from methyl 2-sulfoalkanoates[5] by neutralization with the corresponding metal hydroxide and were purified by recrystallization three

† On leave from the Material Science Research Center, Lion Corp.

Table 1 Molecule numbering for MSAs

Compounds	Numbering
Methyl 2-sulfotetradecanoate sodium salt	**1**
Methyl 2-sulfododecanoate potassium salt	**2**
Methyl 2-sulfotetradecanoate potassium salt	**3**
Methyl 2-sulfohexadecanoate potassium salt	**4**
Methyl 2-sulfooctadecanoate potassium salt	**5**
Methyl 2-sulfotetradecanoate cesium salt	**6**

times from water–ethanol (5:95) solution. The solutions for production of single crystals were screened for a number of combinations of alcohols including one to four carbon atoms in a molecule with various concentrations of water and MSA salts.

Large crystals of **1**–**6** were obtained from the solutions given in Table 2 and were cut into a suitable size for X-ray measurements. Lattice constants and intensity data were measured at room temperature on an Enraf–Nonius CAD4 instrument and a Bruker SMART diffractometer with graphite-monochromated Cu-Kα and Mo-Kα radiation, respectively. The crystal data ‡ and a summary of experimental details are listed in Table 2. The unit cell parameters were refined with 25 reflections in the 2θ range from 40 to 50° on CAD4 and all intensity data on SMART, respectively. Intensity data were collected up to 150 and 52–60° in the 2θ angle on CAD4 and SMART, respectively. The structures were determined by the direct method using the program SHELX-S[26] and were refined by the full-matrix least-squares method using SHELX-L[26] with F_o^2. Hydrogen atoms were refined with a riding model for methyl, methylene and methine groups at estimated positions with isotropic temperature factors multiplied by 1.5, 1.2 and 1.2 to the temperature factors of the attached carbon atoms and were included in the least-squares calculation. Hydrogen atoms in water molecules were picked in different Fourier maps and were included in the refinement with geometrical restraint with fixed OH bond lengths of 0.97 Å. The refinement converged at *R*-values of 0.0586, 0.0581, 0.0650, 0.0852, 0.0990 and 0.0955 for **1**–**6** respectively, for the data of $|F_o| > 4\sigma(|F_o|)$.

Calorimetry

A Seiko DSC220 differential-scanning calorimeter was used for the thermal analysis. The samples were crystallized from the same solution as used in the preparation of crystals for X-ray analysis. The DSC curves were measured at the scan rate of 2.0 °C min^{-1}. The enthalpy at melting transformation was estimated by the integration of the DSC peak, and the entropy was calculated by eqn. (1), where ΔS, ΔH and T_{mp} are the entropy

$$\Delta S = -\Delta H/T_{mp} \quad (1)$$

of melting transformation, the enthalpy of melting transformation, and the melting temperature, respectively.

Molecular mechanics calculations

The external potential energy for each component of MSA in the crystalline state was estimated by molecular mechanics. The external potentials for the van der Waals force, electrostatic potential and hydrogen bonding energy of MSA in a cell were calculated with CHARMm[27] with a periodic boundary mode. The original force parameters were used for the calculations and atomic partial charges were assigned by charge templates in QUANTA 97. The same values of the parameters were used for the anionic molecules of different salts. The cutoff distances in applying the switching function for the calculations of the van der Waals force, electrostatic potential energy, and hydrogen bonding energy were adjusted to 12, 12, and 3.5 Å, respectively.

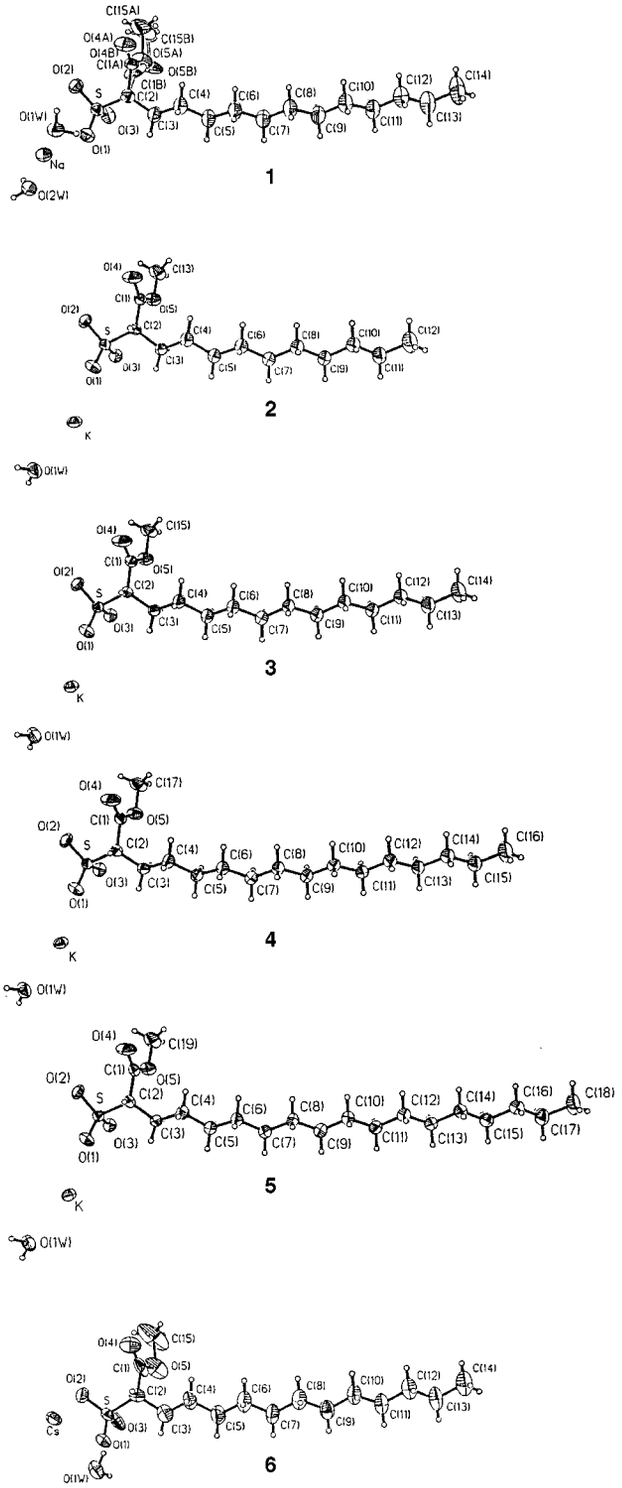

Fig. 1 Molecular structure and atomic numbering for MSA salts, **1**–**6**. Thermal ellipsoids are drawn at 50% probability.

Results

Molecular structures

The molecular structures of **1**–**6** are shown in Fig. 1. The alkyl chain extended from C(2) has an all-*trans* conformation. The

‡ Full crystallographic details, excluding structure factor tables, have been deposited at the Cambridge Crystallographic Data Centre (CCDC). For details of the deposition scheme, see 'Instructions for Authors', *J. Chem. Soc.*, *Perkin Trans. 2*, available *via* the RSC web page (http://www.rsc.org/authors). Any request to the CCDC for this material should quote the full literature citation and the reference number 188/146.

Table 2 Summary of experimental details for **1**–**6**

Compound number	**1**	**2**	**3**	**4**	**5**	**6**
Molecular formula	$C_{15}H_{29}SO_5Na{\cdot}2H_2O$	$C_{13}H_{25}SO_5K{\cdot}H_2O$	$C_{15}H_{29}SO_5K{\cdot}H_2O$	$C_{17}H_{33}SO_5K{\cdot}H_2O$	$C_{19}H_{37}SO_5K{\cdot}H_2O$	$C_{15}H_{29}SO_5Cs{\cdot}H_2O$
Mol. wt.	380.5	350.5	378.6	406.6	434.7	472.4
Solution	iPa–water	nPA–water	nPA–water	nPA–water	nPA–water	EtOH–water
conditions	95 : 5 1 wt%	85 : 15 1.25 wt%	95 : 5 1 wt%	8 : 2 1 wt%	8 : 2 1 wt%	7 : 3 5 wt%
	10 °C	4 °C	r.t.	r.t.	r.t.	r.t.
Crystal size/mm	0.3 × 0.3 × 0.1	0.4 × 0.15 × 0.05	0.4 × 0.25 × 0.05	0.5 × 0.25 × 0.05	0.3 × 0.3 × 0.05	0.2 × 0.1 × 0.02
Crystal system	Orthorhombic	Orthorhombic	Orthorhombic	Orthorhombic	Orthorhombic	Orthorhombic
Space group	*Pbca*	*Pbca*	*Pbca*	*Pbca*	*Pbca*	*Pbca*
a/Å	9.973(4)	10.318(3)	10.313(1)	10.317(2)	10.266(1)	9.867(1)
b/Å	7.596(2)	6.969(1)	7.006(1)	7.027(1)	7.036(1)	7.674(1)
c/Å	55.76(2)	49.81(1)	55.147(1)	60.252(1)	65.229(2)	56.506(1)
Cell volume/Å^3	4224.1	3581.1	3984.1	4368.1	4711.8	4728.5
D_c	1.197	1.300	1.262	1.240	1.225	1.467
F(000)	1648	1504	1632	1760	1888	1020
Radiation	CuKα	MoKα	MoKα	MoKα	MoKα	MoKα
	40 kV 25 mA	50 kV 60 mA	50 kV 60 mA	50 kV 60 mA	50 kV 90 mA	50 kV 90 mA
μ/mm^{-1}	1.82	0.43	0.40	0.37	0.34	1.85
2θ range/°	$1 \le 2\theta \le 150$	$1 \le 2\theta \le 73$	$1 \le 2\theta \le 61$	$1 \le 2\theta \le 61$	$1 \le 2\theta \le 52$	$1 \le 2\theta \le 56$
	$0 \le h \le 12$	$-16 \le h \le 17$	$-13 \le h \le 14$	$-14 \le h \le 12$	$-12 \le h \le 11$	$-13 \le h \le 12$
	$0 \le k \le 9$	$-11 \le k \le 11$	$-9 \le k \le 7$	$-9 \le k \le 9$	$-8 \le k \le 8$	$-10 \le k \le 9$
	$0 \le l \le 69$	$-45 \le l \le 82$	$-77 \le l \le 78$	$-85 \le l \le 72$	$-75 \le l \le 47$	$-75 \le l \le 63$
Data collecting temp.	r.t.	r.t.	r.t.	r.t.	r.t.	r.t.
No. reflections measured	5017	53 319	37 195	20 654	42 304	39 373
No. reflections after merging	5017	8533	5997	6100	4191	5284
R_{int}	—	0.037	0.044	0.047	0.058	0.095
No. reflections observed as						
($\|F_o\| > 4\sigma(\|F_o\|)$)	3615	4101	4937	4145	2977	2526
Scan mode	$\omega/2\theta$	—	—	—	—	—
$\Delta\omega$	$0.80 + 0.15 \times \tan\theta$	—	—	—	—	—
Detector distance/cm	—	5.0	6.0	6.0	6.0	6.0
*R*1						
$\|F_o\| > 4\sigma(\|F_o\|)$	0.0586	0.0581	0.0650	0.0852	0.0990	0.0955
All	0.0676	0.1504	0.0804	0.1288	0.1483	0.1889
*wR*2	0.1654	0.1819	0.1379	0.2439	0.1800	0.1502
No. parameters refined	266	196	214	232	250	215
$\Delta\rho$ excursions/e Å^{-3}	0.5; −0.6	0.3; −0.4	0.3; −0.4	0.4; −0.5	0.3; −0.4	0.8; −0.8

Table 3 The torsion angles in the ester group

Compound no.	**1**		**2**	**3**	**4**	**5**	**6**
Alkyl chain length	13		11	13	15	17	13
Cation	Na^+		K^+	K^+	K^+	K^+	Cs^+
Torsion angles	Part A	Part B					
S(1)–C(2)–C(1)–O(4)	104	91	100.0(3)	99.8(5)	99.8(5)	99.4(6)	94(2)
S(1)–C(2)–C(1)–O(5)	−75	−80	−80.1(2)	−80.9(4)	−80.9(4)	−80.9(5)	−87(1)
C(3)–C(2)–C(1)–O(4)	−128	−151	−134.4(3)	−134.3(5)	−134.3(5)	−134.7(6)	−139(2)
C(3)–C(2)–C(1)–O(5)	51	80	45.5(3)	45.1(5)	45.1(5)	45.0(6)	39(1)
C(2)–C(1)–O(4)–C(ME)	174	172	178.1(2)	178.2(4)	178.2(4)	178.6(4)	176(1)

Table 4 Structural parameters of crystal bilayers for **1**–**6**

Compound number	Alkyl chain length	Thickness/Å			Volume/Å^3 molecule^{-1}		Inclination angle of alkyl chain/°	Σ/Å^2	S/Å^2
		Bilayer	Hydrophobic layer	Hydrophilic layer	Hydrophobic layer	Hydrophilic layer			
1	13	27.9	19.8	8.1	374.9	153.1	1.8	18.9	37.9
2	11	24.9	17.3	7.6	311.1	136.7	2.2	18.0	36.0
3	13	27.6	19.8	7.6	360.3	137.7	1.3	18.0	36.1
4	15	30.1	22.4	7.6	407.7	138.3	2.5	18.2	36.4
5	17	32.6	25.0	7.6	452.5	137.6	1.1	18.0	36.1
6	13	28.3	19.9	8.4	378.5	159.2	1.8	18.9	37.9

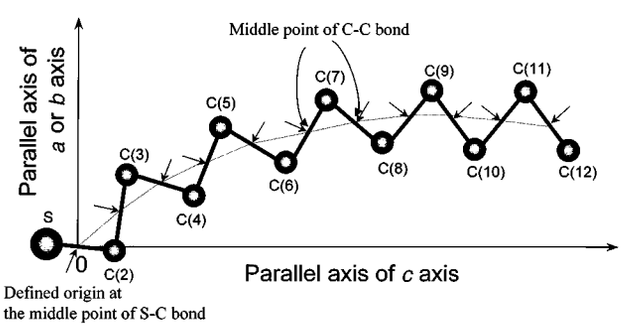

Fig. 2 Schematic drawing of bent alkyl chain. The orthogonal coordinates of the middle points of C–C bonds of the alkyl chains originating at the middle point of the S-C bonds are represented by the bend of the chains. x and z axes are parallel to a and c axes of the cell, respectively. The arrows indicate the middle points of each bond.

sulfur atom is located at the terminal of the alkyl chain. The ester group is branched as a side chain at C(2) linking the alkyl chain and sulfonato group. The ester group of MSA·Na is disordered, and that of MSA·Cs has relatively large temperature factors. The torsion angles around the ester group shown in Table 3 are slightly different between the crystals of MSA·Na and MSA·Cs salts, but those of MSA·K salts are the same among the crystals of anions with a variety of alkyl chain lengths. The alkyl chains are bent as illustrated in Fig. 2, because of the bulkiness of the adjacent molecules. The x, y and z components of the vector from the middle point of the S–C(2) bond to each main chain atom are plotted in Fig. 3. Alkyl chains are more bent near the sulfonato group than near the terminal. The alkyl chain of MSA·Na draws a curve slightly different from MSA·K salts. The bending of the alkyl chain has also been observed in the crystals of glycolipids.[11]

The crystals of MSA·Na, MSA·K and MSA·Cs salts contain two, one, and one water molecules for each anionic molecule, respectively. In contrast, the reported number of water molecules in SDS crystals is $\frac{1}{8}$, $\frac{1}{4}$, $\frac{1}{2}$ and 1.[9]

Crystal structures

The crystal structures of **1**–**6** are shown in Fig. 4. The anions have a stereogenic carbon atom, C(2), connecting the sulfonato, ester and alkyl groups as shown in Fig. 5. The crystal includes both of the enantiomers and forms racemic compounds. The enantiomers in the crystal of **2** are shown in Fig. 6.

The crystal structures of amphiphiles are categorized into three types, a monolayer structure and two bilayer structures with the terminals of the alkyl chain facing each other in a plane of cleavage (Type F) and interdigitated alkyl chains (Type I) as shown in Fig. 7. The MSA molecules are arranged to form a bilayer structure with interdigitated alkyl chains in a two-by-two mode (Type I-2), shown in Fig. 4. The two anions encountered in a unit are enantiomeric to each other. Interdigitated structures with one-by-one alkyl chains (Type I-1) have been reported for glycolipids which have pyranosides,[11–15] and trimethylammonium chlorides.[25] The unit structure of two-by-two alkyl chains has been reported only for *N*-*n*-octyl-6-deoxy-D-gluconamide.[28] The arrangements of the anions in the crystal are schematically shown in Fig. 8 in comparison with the one-by-one unit structure.

The crystal structure consists of two layers, hydrophobic and hydrophilic. The hydrophobic layer is formed by sulfonato groups, cations and water molecules, while the hydrophobic layer is formed by the alkyl chains. Parameters describing the thickness and volumes of hydrophobic and hydrophilic layers, the inclinations of alkyl chains, and the occupied area of the alkyl chains and hydrophilic heads in a layer are shown in Table 4. Hydrophobic and hydrophilic layers are separated at the C(2) atom. The thickness and volume of the hydrophobic layer are slightly different among crystals of MSA·Na, **1**, MSA·K, **3**, and MSA·Cs, **6**, which have the same length of alkyl chain. The volumes of the hydrophobic layers of MSA·Na, **1**, and MSA·Cs, **6**, are larger than those of MSA·K, **3**, because of the loose packing of the alkyl chains of MSA·Na and MSA·Cs as indicated by the occupied area of alkyl chains, 18.9, 18.9 and 18.1 Å^2 for each alkyl chain of MSA·Na, MSA·Cs and MSA·K salts, respectively. The hydrophilic layer of the MSA·Na, **1**, has a larger volume and greater thickness than that of the MSA·K, **3**, because the MSA·Na has two water molecules instead of one water molecule as in **3**. The hydrophilic layer of the MSA·Cs, **6**, also has a larger volume and greater thickness than that of the MSA·K because of the larger radius of the cesium ion than the potassium ion. The effect of the alkyl chain length is slight in MSA·K salts on the crystal packing. The occupied areas of the hydrophilic head of MSA·Na and MSA·Cs are slightly

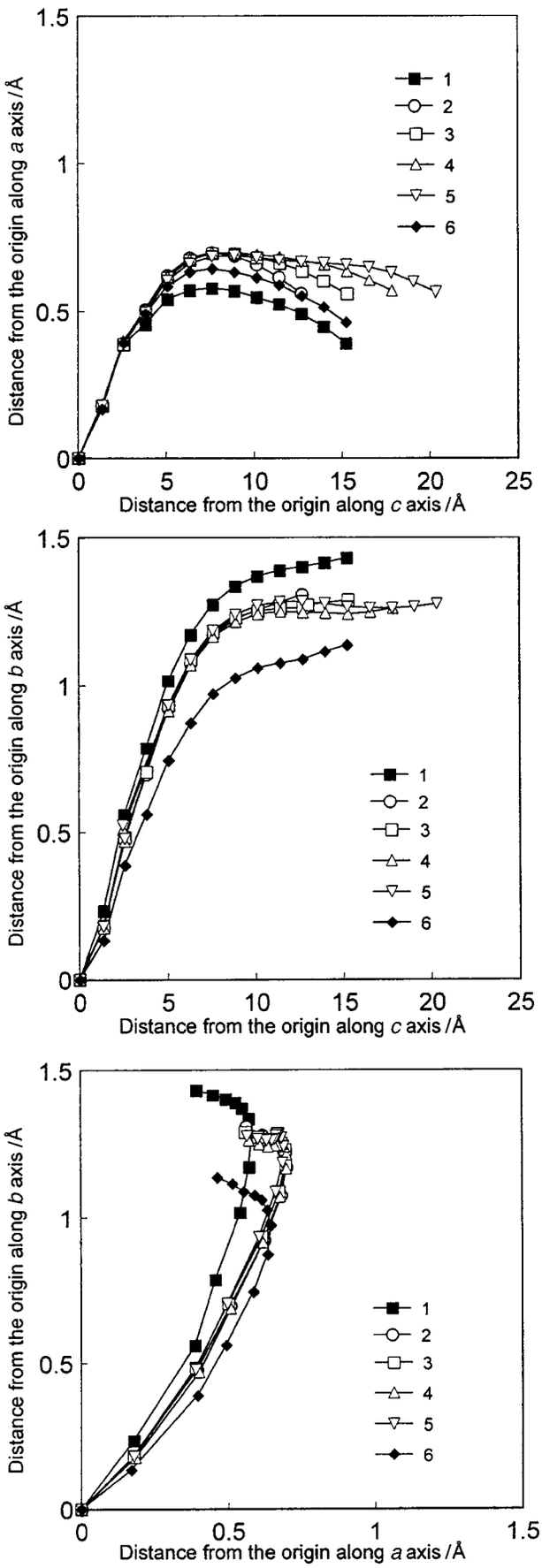

Fig. 3 Shape of the alkyl chain. The coordinates of the middle point of the C–C bond in the alkyl chain are defined in Fig. 2.

larger than those of MSA·K salts. The occupied area of the hydrophilic head in each crystal is twice that of the alkyl chain.

Packing of the hydrophilic layers

The packing of the hydrophilic layers is shown in Fig. 9. Each cation has a different coordination structure and contact distance between the oxygen atoms of the sulfonato group and water molecules. The coordination of the hydrophilic heads, cations, and water molecules is shown in Fig. 10–12. The contact distances between the cation and oxygen atoms are listed in Table 6. The coordination number of the sodium, potassium and cesium ions is six, six and nine, respectively. The sodium, potassium, and cesium ions are in contact with two, four and six oxygen atoms of the sulfonato groups, respectively, and also with four, two and three oxygen atoms of the water molecules, respectively. The sodium ion is in contact with two anionic molecules in the same layer but does not link the two layers. In contrast, the potassium ion links two anionic molecules in the same layer and an anionic molecule of the adjacent layer while the cesium ion is in contact with three anionic molecules in the same layer and an anionic molecule of the adjacent layer. The distances of coordination from sodium, potassium and cesium ions to oxygen atoms are 2.37–2.45, 2.69–2.99 and 3.00–3.51 Å, respectively, which are affected by the ionic radius of each cation. The sulfonato group binds two cations and three water molecules, four cations and two water molecules, and four cations and four water molecules in the crystals of MSA·Na, MSA·K and MSA·Cs salts, respectively. The ester group of MSA·Na binds one water molecule at the carbonyl oxygen, O(4), with hydrogen bonding, and that of MSA·Cs is in contact with a cesium ion. The numbers of ionic bondings between cation and anion in the crystals of MSA·K and MSA·Cs are greater than that of the sodium salt.

One water molecule in MSA·Na and the water molecule in MSA·K salts form bifurcated hydrogen bonds with two sulfonato groups forming a bridge and in contact with two cations in the tetrahedral direction. Another water molecule of the crystal of MSA·Na binds oxygen atoms of the sulfonato group and carbonyl group by hydrogen bonding and is in contact with two sodium ions in a tetrahedral arrangement. The water molecule of the crystal of MSA·Cs also forms a bridge to two sulfonato groups, and the oxygen atom is in contact with three cesium ions. The geometry of the hydrogen bonding and the coordination of the cations are listed in Tables 5 and 6, respectively.

Packing of the alkyl chain

The tilt angle of the *c* axis and least-squares line of the middle points between neighboring carbon atoms in the alkyl chain higher than 5 is 1.6°. The arrangement of the alkyl chain is shown in Fig. 13. The packing type of the alkyl chain is $O_{\perp}$, which was categorized by Vand,[29] and the subcell constant is shown in Table 7.

The occupied areas of the alkyl chain in MSA·Ks are smaller than those in MSA·Na and MSA·Cs. The alkyl chains are bent as shown in Fig. 3, which may be caused by the contacts of the adjacent molecules in the crystal. The magnitude of the bending is shown in Fig. 3. This bending is caused by the repulsion between bulky groups, the ester group and especially the sulfonato group.

Atomic temperature factors

The values of isotropic temperature factors reproduced from the anisotropic temperature factors for **1**–**6** are shown in Fig. 14. The isotropic temperature factors of the alkyl chains exhibit thermal motion greater than those of the sulfonato group. The isotropic temperature factors of the sulfonato group for MSA·K are slightly smaller than those of the sodium and cesium salts. The oxygen atom, O(3), in the sulfonato group of MSA·Na and MSA·Cs, bound to only water molecules, has a temperature factor larger than that of the other two oxygen

Table 5 Contact distances between metal ion and oxygen atoms

Compound number	1			6		
	Atoms with symmetry operation		Distances/Å	Atoms with symmetry operation		Distances/Å
	Na[x, y, z]	O1[x, y, z]	2.453	Cs[x, y, z]	O1[x, y, z]	3.254
		O2[0.5 − x, −0.5 + y, z]	2.378		O1[−0.5 − x, 0.5 + y, z]	3.042
		O1W[x, y, z]	2.384		O2[x, y, z]	3.356
		O1W[−x, 1 − y, z]	2.543		O2[−0.5 + x, 1.5 − y, −z]	3.325
		O2W[x, y z]	2.373		O2[0.5 + x, 0.5 − y, −z]	2.995
		O2W[0.5 − x, 0.5 + y, z]	2.418		O4[0.5 + x, 0.5 − y, −z]	3.321
					O1[−0.5 + x, 1 + y, −0.5 − z]	3.282
					O1W[−0.5 + x, 0.5 − y, −z]	3.513
					O1W[−0.5 − x, 0.5 + y, z]	3.292

Compound number		2	3	4	5
Atoms with symmetry operation		Distances/Å			
K [x, y, z]	O1[x, y z]	2.686	2.696	2.700	2.692
	O1[0.5 − x, −0.5 + y, z]	2.773	2.779	2.786	2.783
	O2[x, −1 + y, z]	2.751	2.761	2.771	2.777
	O2[1 − x, 1 − y. −z]	2.815	2.819	2.819	2.822
	O1w[x, y z]	2.823	2.835	2.835	2.988
	O1w[0.5 − x, 0.5 + y, z]	2.953	2.971	2.985	2.988

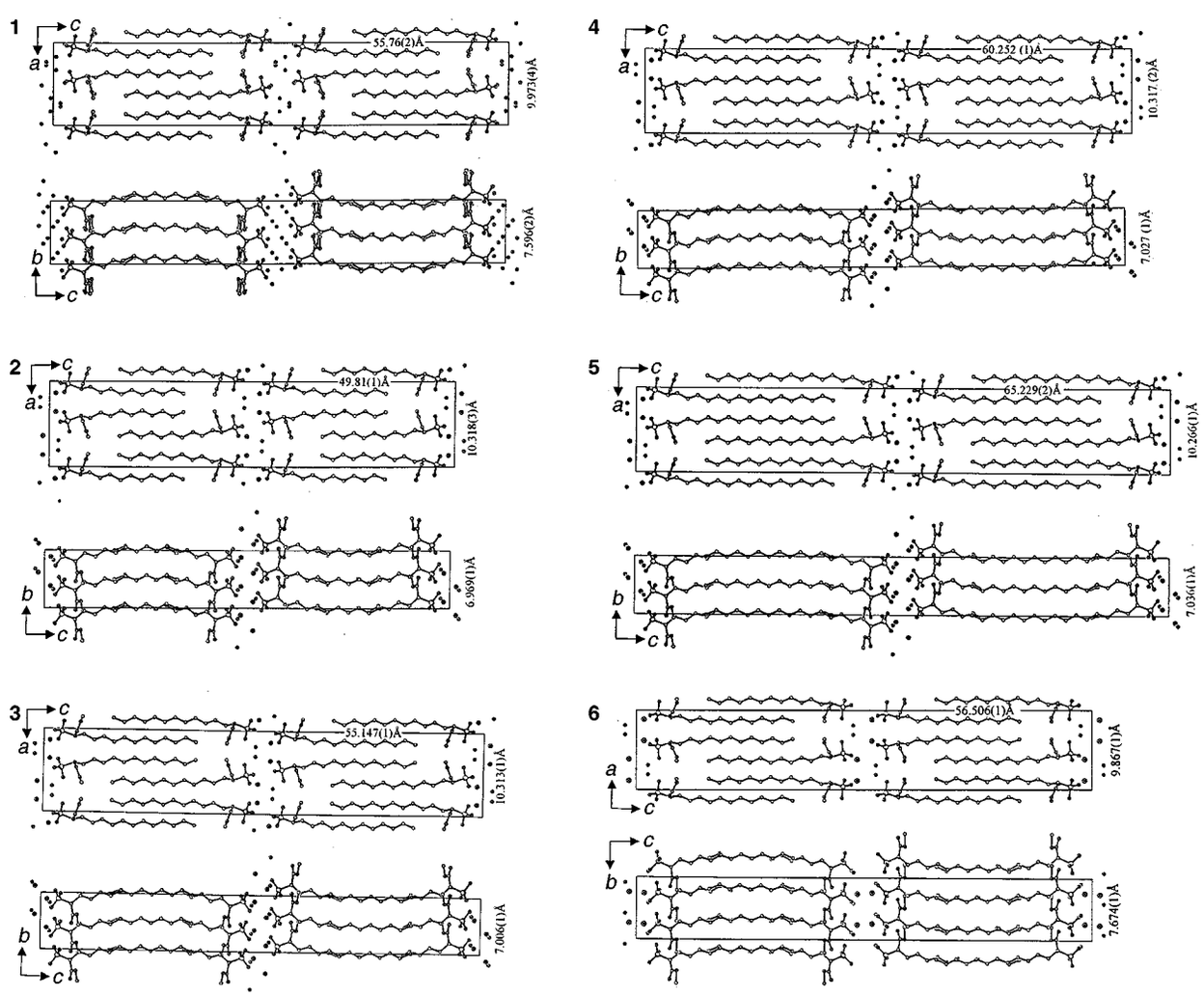

Fig. 4 The crystal structures of MSA salts, **1**–**6**, projected on *ac* and *bc* planes.

atoms, O(1) and O(2), bound to the cations. The temperature factor of the O(3) atom is decreased in the order of those for MSA·Cs, MSA·Na and MSA·K. The temperature factors are relatively large at the end of the alkyl chain. The terminal carbon atoms of the alkyl chain and the ester group located close by have relatively large thermal motion, as shown in Fig. 15. The temperature factors of the alkyl chain of MSA·Na and MSA·Cs are larger than those of the MSA·K salts. The ester

Table 6 Hydrogen bonding geometry of water molecules in the crystals of **1**–**6**

Compound no.	Acceptor A1	Acceptor A2	Donor oxygen atom of water molecule	Hydrogen bonding distances/Å and angles/° A1···H	A1···O	∠A1–H–O	A2···H	A2···O	∠A2–H–O
1	O(1) 1[a]	O(4A) 2[a]	O(1W) 3	1.97	2.91	164	2.21	3.17	178
		O(4B) 2[a]	O(1W) 3	—	—	—	2.11	3.05	164
	O(2) 4[a]	O(3) 5[a]	O(2W) 3	1.92	2.86	165	1.88	2.81	161
2	O(3) 6[a]	O(3) 5[a]	O(1W) 3	2.02	2.90	166	1.91	2.85	169
3	O(3) 6[a]	O(3) 5[a]	O(1W) 3	2.01	2.90	166	1.94	2.85	167
4	O(3) 6[a]	O(3) 5[a]	O(1W) 3	1.96	2.9	172	1.92	2.86	165
5	O(3) 6[a]	O(3) 5[a]	O(1W) 3	1.96	2.90	174	1.93	2.85	165
6	O(3) 3[a]	O(3) 2[a]	O(1W) 3	1.86	2.84	178	1.93	2.88	168

[a] 1; [0.5 − x, 0.5 + y, z], 2; [0.5 − x, −0.5 + y, z], 3; [x, y, z], 4; [1 − x, 1 − y, −z], 5; [−0.5 + x, 0.5 − y, −z], 6; [1 − x, −y, −z].

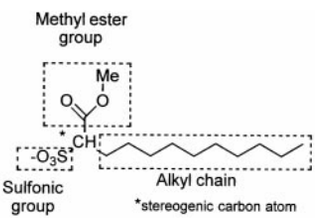

Fig. 5 Schematic representation of the chemical structure of MSA.

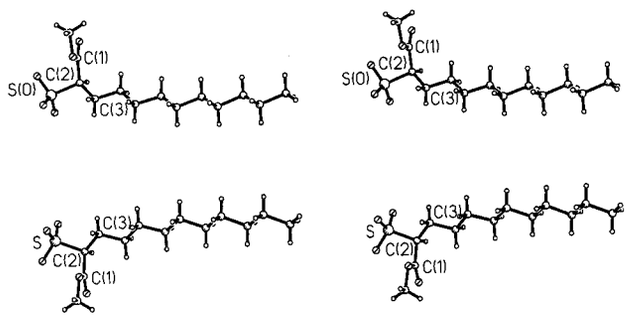

Fig. 6 Stereodrawing of enantiomers of MSA·K, **2**, in the crystal.

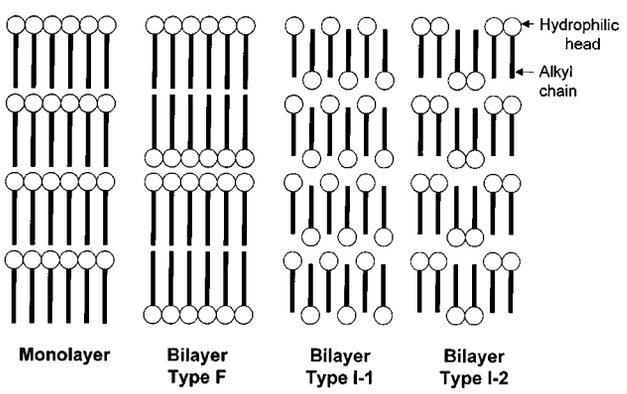

Fig. 7 Schematic drawing of the arrangement of amphiphiles. Types F, I-1, and I-2 have arrangements of a hydrophobic layer of the chain terminals facing in planes of cleavage, of one-by-one, and of two-by-two interdigitated alkyl chains.

group of MSA·Cs has temperature factors larger than those of the other MSA especially for the O(5) atom.

Calorimetry

Melting temperatures, enthalpy and entropy of melting transitions are shown in Table 8. At melting temperature, the direct transition from crystal to isotropic liquid is observed by polarized microscopy. The melting point of MSA·K is the highest among the MSAs for three types of cations and the same length of alkyl chain, and that for MSA·Cs is higher than that for the MSA·Na. Crystals of MSA·K salts with longer alkyl chains

Table 7 Cell constant[a] of subcell for the packing of the alkyl chain

Compound no.	a/Å	b/Å	c/Å
1	4.987	7.596	2.544
2	5.157	7.006	2.552
4	5.159	7.036	2.553
5	5.113	7.036	2.549
6	4.994	7.674	2.539

[a] Type of cell is $O_{\perp}$, and $\alpha = \beta = \gamma = 90°$.

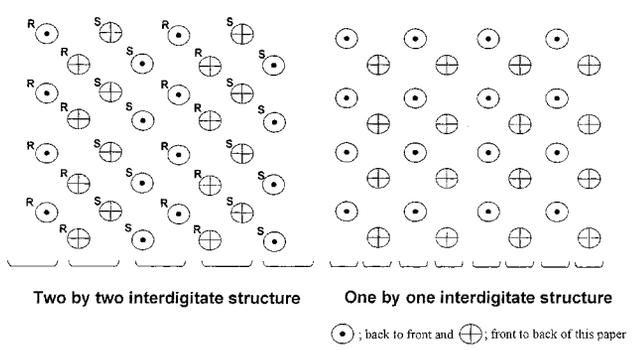

Fig. 8 Arrangement of alkyl chains viewed along the direction of the molecule perpendicular to the *ab* plane.

have higher melting points. MSA·Na, **1** has the greatest value of melting enthalpy and entropy change among the MSAs having the same length of alkyl chain, and the MSA·K, **3** has a melting enthalpy value greater than the MSA·Cs, **6**.

Packing energy

(i) Internal energy. Internal energy was estimated from the sum of the energy terms, bonding, bond-angle, torsion angle, and improper torsion angle.[27] The total internal energy is listed in Table 9. Because the bonding distances and angles obtained from X-ray data are different from those of the ideal structures, the internal energy calculated from the X-ray coordinates is greater than that calculated with the ideal structure. The internal energy of an anionic molecule in the crystal was estimated from the idealized structure in the cell by energy minimization, by sequentially: locating eight anionic molecules with corresponding cations and water molecules in a cell, setting atomic constraints for seven anionic molecules and all of the cations and water molecules, setting a periodic boundary for the cell, executing minimization, and extracting internal energy for the minimized molecule. The positive internal energy of the anion in the cell, 9–12 kJ mol^{-1}, shown in Table 9, is caused by the distortion of the molecule in the crystalline state, especially by the bending of the alkyl chain.

(ii) Energy terms of external energy. The packing energy was estimated with energy calculation by molecular mechanics in the static state. External energy, E_{ex} is calculated from eqn.

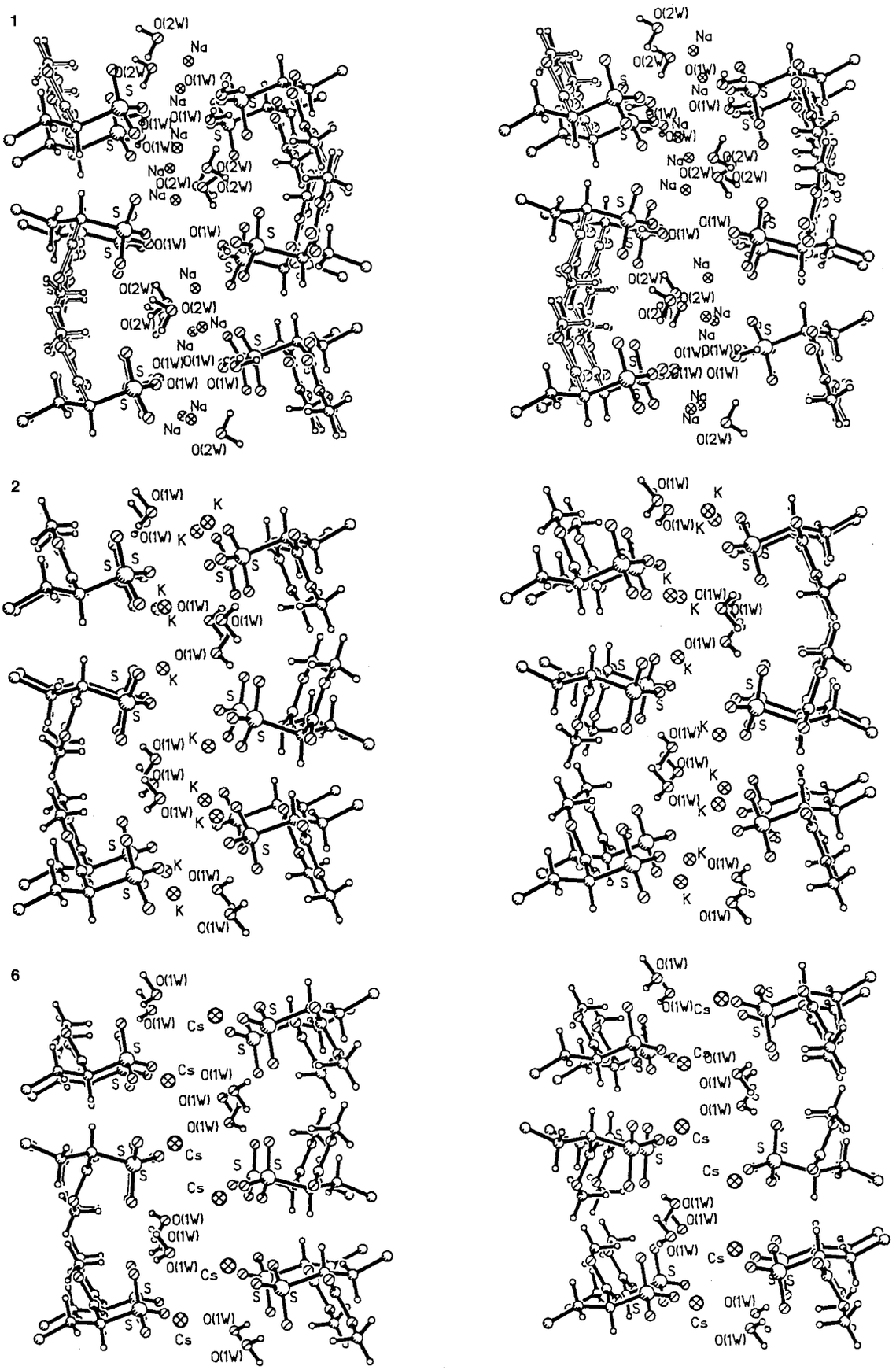

Fig. 9 Stereo views of the packing of hydrophilic layers parallel to the *ac* plane.

(2),[27] where E_{esp} is the electrostatic potential and E_{vdw} is the Lennard-Jones potential for the van der Waals force.

$$E_{ex} = E_{esp} + E_{vdw} \quad (2)$$

The hydrogen bonding energy is calculated as part of the electrostatic potential and van der Waals force. However, the contribution of hydrogen bonding energy in the objective molecular system is estimated and extracted by eqn. (3)[27] where

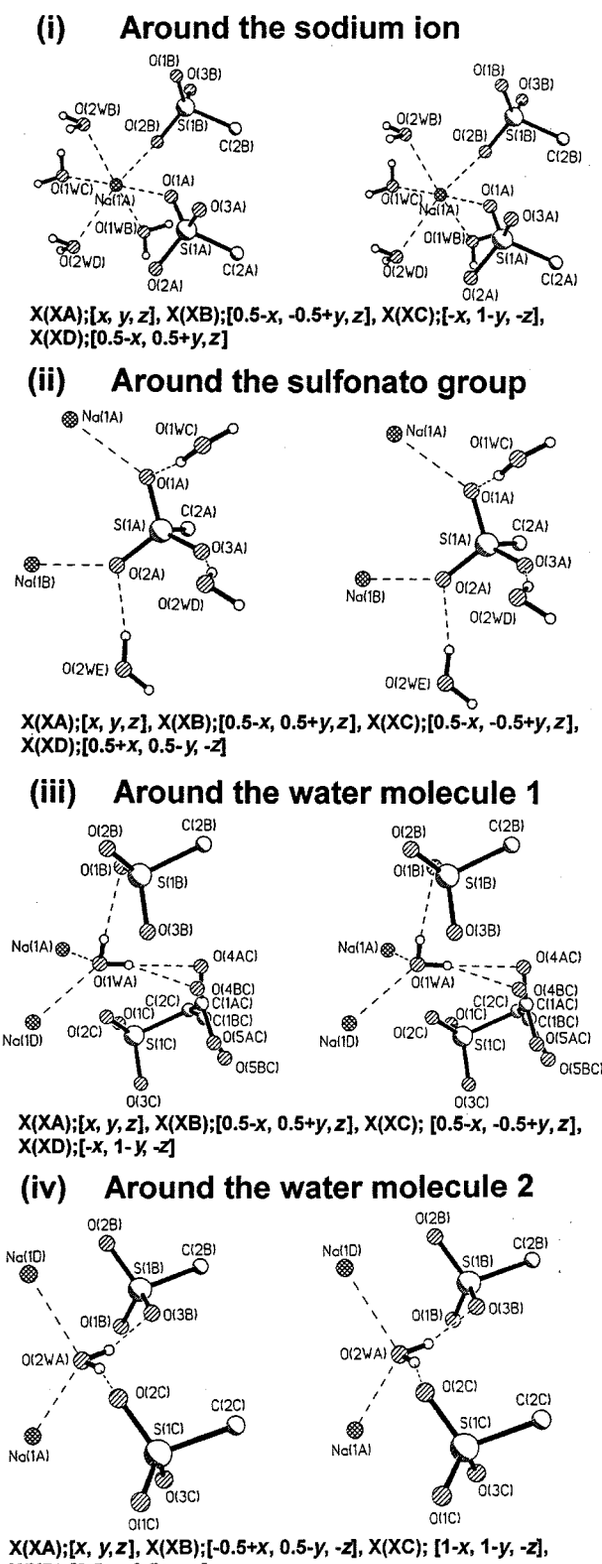

Fig. 10 Contacts of cations, sulfonato groups, and water molecules for MSA, **1**.

$$E_{hy} = \Sigma[(C_{kl}/r_{ADkl}^{6}) - (D_{kl}/r_{ADkl}^{4})]\cos^{m}(\varphi_{A-H-D})\cos^{n}(\varphi_{AA-A-H}) \quad (3)$$

r_{ADkl} is the atomic distance between the hydrogen donor atom, k, and acceptor atom, l; C_{kl} and D_{kl} are the same types of parameters with the van der Waals force; m and n are (0,2,4) and (0,2), respectively, determined by the hydrogen bonding geometry; and φ_{A-H-D} and φ_{AA-A-H} are hydrogen bonding angles for acceptor oxygen atom (A), donor hydrogen atom (H), and donor oxygen atoms (D), and atoms bound to the acceptor atom (AA), acceptor oxygen atom (A) and the donor hydrogen atoms (H).

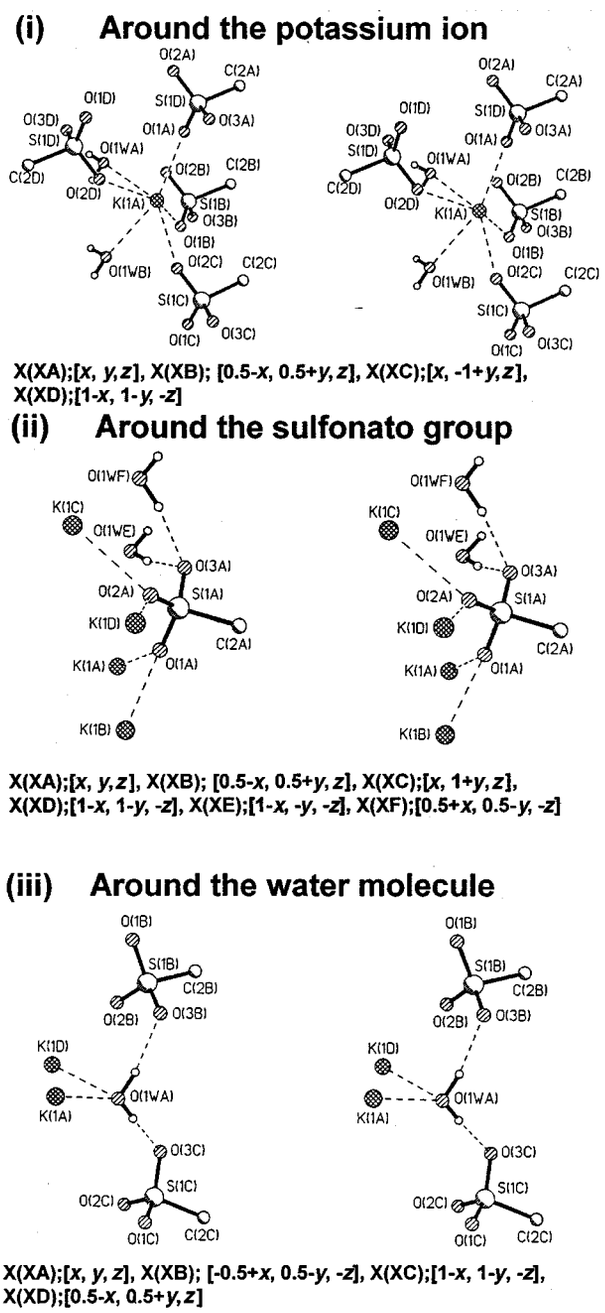

Fig. 11 Contacts of cations, sulfonato groups, and water molecules for MSA, **3**.

The total packing energies of the crystal, $E_{all,tot}$ listed in Table 10 and estimated from the terms of the external energy given by eqn. (4), where $E_{esp,tot}$ and $E_{vdw,tot}$ are the electrostatic potential

$$E_{all,tot} = E_{esp,tot} + E_{vdw,tot} \quad (4)$$

and van der Waals force, respectively, for all of the components located at the crystal coordinates. The values of $E_{tot,all}$ for the sodium and cesium salts are the highest and lowest in the three types of salts having the same length of alkyl chain of anions, and those of MSA·K salts are increased with increasing length of the alkyl chain.

(iii) Calculation of energy values for each component. The potential energies in the crystals for each component, E_A, E_C and E_W, and for the combinations, the anions and the cations,

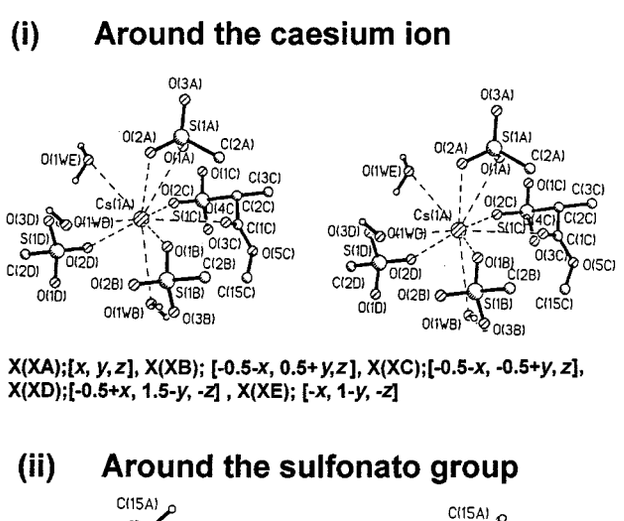

Fig. 12 Contacts of cations, sulfonato groups, and water molecules for MSA, **6**.

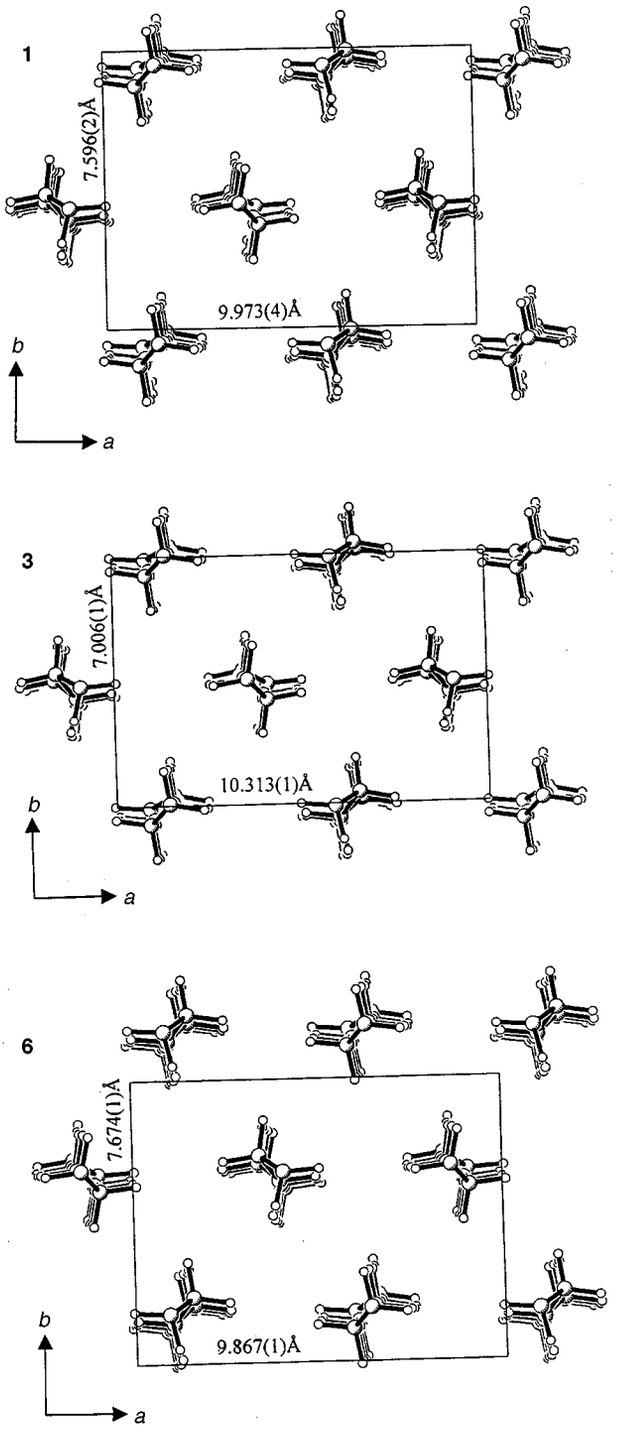

Fig. 13 Arrangement of alkyl chains in MSAs, **1**, **3** and **6**, parallel to the *ab* plane.

E_{AC}, the anions and the water molecules, E_{AW}, the cations and water molecules, E_{CW}, are calculated. The external energies of E_{A0}, E_{C0} and E_{W0} of the isolated components, an anion, a cation, a water molecule for MSA·K and MSA·Cs or two water molecules for MSA·Na, respectively, are zero. When the components built a crystal, each component had external energy, E_A, E_C and E_W for the crystal of the anion, for the crystal of the cation, and for the crystal of the water molecule, respectively. In the crystal, the components interact with each other, and the contribution of each component to $E_{all,tot}$ is different for each combination, anion and cation, ΔE_{AC}, anion and water molecule, ΔE_{AW}, and cation and water molecule, ΔE_{CW}, which are expressed in eqns. (5)–(7). The relationship among the

$$\Delta E_{AC} = E_{AC} - E_A - E_C \quad (5)$$

$$\Delta E_{AW} = E_{AW} - E_A - E_W \quad (6)$$

$$\Delta E_{CW} = E_{CW} - E_C - E_W \quad (7)$$

and

$$E_{tot} = E_A + E_W + E_C + \Delta E_{AC} + \Delta E_{AW} + \Delta E_{CW} \quad (8)$$

energy terms is shown in Fig. 16. The values of E_A, E_W, E_C, ΔE_{AC}, ΔE_{AW} and ΔE_{CW} with each energy term are listed in Table 11.

E_C has a larger value, 2189–2349 kJ mol^{-1} than E_A, 1684–1914 kJ mol^{-1}, and E_W, −2–15 kJ mol^{-1}, is the lowest of these three terms. E_C and E_A are mostly affected by the electrostatic potential caused by the repulsion between the inter-positive or inter-negative charges, respectively. ΔE_{AC} is the lowest among ΔE_{AC}, ΔE_{AW} and ΔE_{CW} and has the largest effect on reducing $E_{all,tot}$, because of the strong interaction between negative and

positive charges. Therefore ΔE_{AC} is the most important term to stabilize the crystal among ΔE_{AC}, ΔE_{AW} and ΔE_{CW}. ΔE_{AW} has a small and positive value, 43–66 kJ mol^{-1}, which does not contribute to the reduction of $E_{all,tot}$ in spite of the negative values of hydrogen bonding energy estimated by eqn. (3) which are in the range −61 to −31 kJ mol^{-1}. ΔE_{CW} with a medium value, −302 to −148 kJ mol^{-1}, effects a decrease in $E_{all,tot}$. The values of ΔE_{AW} and ΔE_{CW} indicate that the water molecule plays a role in stabilizing the cations, and there is a relatively small effect to stabilize anionic molecules. The effect of the alkyl chain on stabilizing the crystal is estimated from $E_{A,vdw}$ as −190 to −108 kJ mol^{-1}, which contributes to assembling the anions and reducing $E_{all,tot}$.

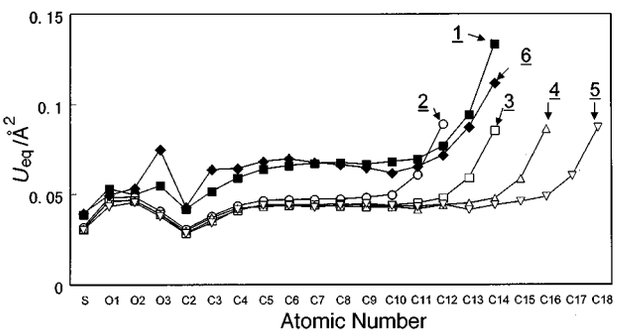

Fig. 14 Plot of isotropic temperature factors for atoms in the alkyl chain and sulfonato group of MSAs, **1**–**6**.

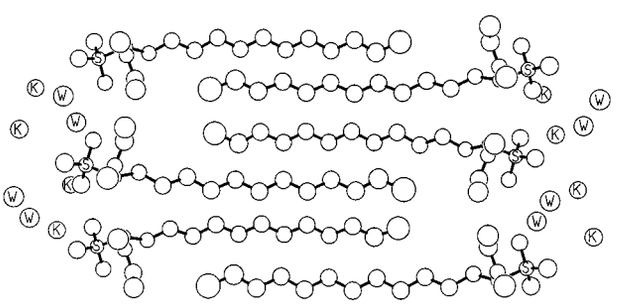

Fig. 15 Thermal motion of MSA·K in a layer. Thermal spheroids of U_{eq} were drawn at 80% probability.

Table 8 The melting point, the enthalpies and entropies of **1**–**6**

Compound number	Mp/°C	ΔH/10^{-1} kJ mol^{-1}	ΔS/10^{-2} mol^{-1} K^{-1}
1	54.1	−5.15	1.57
2	67.6	−3.89	1.14
3	75.9	−4.94	1.41
4	81.9	−5.73	1.61
5	87.2	−6.49	1.79
6	67.8	−4.44	1.29

(iv) Characteristics of the components in the different crystals. *Cations.* The crystals having different cations have characteristic values for each energy term. The electrostatic potential between ions, especially reflected by the values of $\Delta E_{AC,esp}$, is the lowest for the potassium salts, and the highest for the cesium salts. A potassium ion is in contact with four sulfonato groups in the crystal and effects a greater reduction in $\Delta E_{AC,esp}$ than a sodium ion in contact with two sulfonato groups. The cesium ion is in contact with five oxygen atoms of four sulfonato groups, but does not reduce $\Delta E_{AC,esp}$ because the distances between the cesium ion and oxygen atom of the sulfonato groups, 3.0–4 Å, are greater than those of the sodium ion, 2.4–5 Å, and the potassium ion, 2.7–8 Å. Those differences in the distances are caused by the ionic radii of the cations, 1.13, 1.52 and 1.81 for Na^+, K^+ and Cs^+, respectively.[30]

Anions. The contribution of the interaction between the alkyl chains, reflected in $E_{A,vdw}$, is the greatest for MSA·K salts in the crystals having three types of cations. The values of $E_{A,vdw}$ for the MSA·Na and MSA·Cs are slightly different from each other. The change in $E_{A,vdw}$ depending on the cation is caused by the packing difference in the alkyl chain. In contrast to the value of $E_{A,vdw}$, $E_{A,esp}$ of MSA·Cs is the lowest in the three types of crystals with each cation, and that for the MSA·Na is lower than that of MSA·K, because of the shorter distances between the sulfonato groups.

Hydration. The contribution of hydration to the cations for the total energy of crystal packing, E_{tot}, is represented by the value of $\Delta E_{CW,tot}$ which is the smallest for the sodium salt among the three types of cations, and that for the potassium salts is slightly different from that for MSA·Cs, which is mostly affected by the hydration numbers, two, one, and one respectively for MSA·Na, MSA·K and MSA·Cs salts.

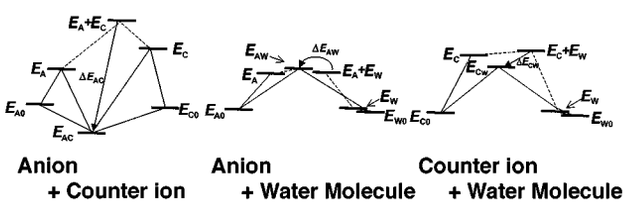

Fig. 16 Schematic view of the energy levels in crystal packings.

Table 10 Total packing energy including terms of electrostatic, Lennard-Jones potentials and hydrogen bonding energy for **1**–**6**

Compound number	Energy terms/10^{-3} kJ mol^{-1}			
	$E_{all,tot}$	$E_{all,esp}$	$E_{all,vdw}$	$E_{all,hb}$
1	−0.809	−0.728	−0.081	−0.061
2	−0.720	−0.629	−0.091	−0.031
3	−0.742	−0.628	−0.114	−0.031
4	−0.773	−0.640	−0.132	−0.032
5	−0.782	−0.630	−0.151	−0.032
6	−0.553	−0.485	−0.067	−0.033

Table 9 Internal energy of the molecules

Compound no.	Values of internal energy/10^{-3} kJ mol^{-1}			
	Original coordinate $E_{i,0}$	Minimized in the cell $E_{i,c}$	Minimum conformation $E_{i,m}$	$E_{i,c} - E_{i,m}$
1 Conformer a	0.784	0.149	0.096	0.053
Conformer b	1.030	—	—	
2	0.672	0.140	0.102	0.038
3	0.749	0.135	0.096	0.039
4	0.830	0.128	0.089	0.039
5	0.911	0.123	0.085	0.038
6	0.911	0.123	0.085	0.038

Table 11 The potential energies [$\times 10^3$ kJ mol^{-1}] between each component

Compound		Combination of components			Each component			Stabilization		
	Total	$E_{AC,tot}$	$E_{AW,tot}$	$E_{CW,tot}$	$E_{A,tot}$	$E_{C,tot}$	$E_{W,tot}$	$\Delta E_{AC,tot}$	$\Delta E_{AW,tot}$	$\Delta E_{CW,tot}$
	ESP	$E_{AC,esp}$	$E_{AW,esp}$	$E_{CW,esp}$	$E_{A,esp}$	$E_{C,esp}$	$E_{W,esp}$	$\Delta E_{AC,esp}$	$\Delta E_{AW,esp}$	$\Delta E_{CW,esp}$
	VDW	$E_{AC,vdw}$	$E_{AW,vdw}$	$E_{CW,vdw}$	$E_{A,vdw}$	$E_{C,vdw}$	$E_{W,vdw}$	$\Delta E_{AC,vdw}$	$\Delta E_{AW,vdw}$	$\Delta E_{CW,vdw}$
	HB	$E_{AC,hb}$	$E_{AW,hb}$	$E_{CW,hb}$	$E_{A,hb}$	$E_{C,hb}$	$E_{W,hb}$	$\Delta E_{AC,hb}$	$\Delta E_{AW,hb}$	$\Delta E_{CW,hb}$
1		*−0.573*	*1.818*	*2.005*	*1.753*	*2.291*	*0.015*	*−4.617*	*0.050*	*−0.302*
		−0.469	1.953	1.959	1.864	2.291	0.016	−4.625	0.073	−0.348
		−0.104	−0.135	0.046	−0.111	−0.000	−0.001	0.008	−0.023	0.046
		0.000	−0.061	0.000	0.000	0.000	0.000	0.000	−0.061	0.000
2		*−0.614*	*1.961*	*2.194*	*1.914*	*2.349*	*−0.002*	*−4.878*	*0.049*	*−0.153*
		−0.513	2.101	2.177	2.045	2.349	−0.001	−4.907	0.056	−0.171
		−0.101	−0.140	0.017	−0.131	0.000	−0.001	0.029	−0.007	0.018
		0.000	−0.031	0.000	0.000	0.000	0.000	0.000	−0.031	0.000
3		*−0.636*	*1.878*	*2.185*	*1.837*	*2.336*	*−0.002*	*−4.887*	*0.044*	*−0.148*
		−0.513	2.038	2.169	1.988	2.335	−0.001	−4.836	0.051	−0.165
		−0.123	−0.160	0.016	−0.151	0.001	−0.001	0.028	−0.007	0.017
		0.000	−0.031	0.000	0.000	0.000	0.000	0.000	−0.031	0.000
4		*−0.660*	*1.829*	*2.164*	*1.782*	*2.323*	*0.001*	*−4.766*	*0.046*	*−0.160*
		−0.518	2.006	2.148	1.952	2.323	0.002	−4.794	0.052	−0.177
		−0.142	−0.177	0.016	−0.170	0.000	−0.001	0.028	−0.006	0.017
		0.000	−0.032	0.000	0.000	0.000	0.000	0.000	−0.032	0.000
5		*−0.667*	*1.791*	*2.178*	*1.746*	*2.336*	*0.001*	*−4.751*	*0.043*	*−0.159*
		−0.506	1.987	2.162	1.936	2.336	0.002	−4.779	0.049	−0.176
		−0.161	−0.196	0.016	−0.190	0.000	−0.001	0.028	−0.006	0.016
		0.000	−0.032	0.000	0.000	0.000	0.000	0.000	−0.032	0.000
6		*−0.456*	*1.757*	*2.028*	*1.684*	*2.189*	*0.008*	*−4.329*	*0.066*	*−0.171*
		−0.376	1.866	2.015	1.792	2.189	0.009	−4.358	0.065	−0.184
		−0.080	−0.109	0.013	−0.108	0.000	−0.001	0.029	0.001	0.013
		0.000	−0.033	0.000	0.000	0.000	0.000	0.000	−0.033	0.000

Energy difference between crystals. The energy terms of MSA·Na, **1** are larger than those of MSA·K, **3**, −67, −84, −45, 17, 190, 6 and −154 kJ mol^{-1} for $E_{all,tot}$, E_A, E_C, E_W, $\Delta E_{AC,tot}$, $\Delta E_{AW,tot}$, $\Delta E_{CW,tot}$, respectively. These differences indicate that the low repulsion energy between the sulfonato groups and between sodium ions contributes to stabilizing the sodium salt by −84 and −45 kJ mol^{-1}, respectively, more than the potassium salts. Hydration of the sulfonato group destabilizes by 6 kJ mol^{-1}. Hydration by one more water molecule of the cation decreased by −154 kJ mol^{-1} more than MSA·K. The electrostatic potential between the water molecules destabilizes the lattice energy by 17 kJ mol^{-1}. The electrostatic potential between the anionic molecule and the cation destabilizes 190 kJ mol^{-1} less than the MSA·K salts. The corresponding energy values for the cesium salt, **6**, are −189, −153, −147, 10, 478, 22 and −23 kJ mol^{-1} for $E_{all,tot}$, E_A, E_C, E_W, $\Delta E_{AC,tot}$, $\Delta E_{AW,tot}$, $\Delta E_{CW,tot}$ and suggest that MSA·Cs is energetically less stable than the potassium salts because of the longer distance to the cation.

Discussion

Interdigitated structures of amphiphiles observed in some crystals in glycolipids[11–15] and alkyl trimethyl halides[25] have been ascribed to the difference of the size between the head group and alkyl chain of the molecule. The occupied area of the hydrophilic head of the molecules in the crystal depends on the structure of the amphiphiles, as 37.9, 39.3, 21.0 and 25.8 Å^2, for the crystals of MSA·Na, **1**, decyl α-D-glucopyranoside (DG).[15] SDS $\frac{1}{8}$ hydrate (SDS·$\frac{1}{8}$H$_2$O),[2] and SDS $\frac{1}{2}$ hydrate (SDS·$\frac{1}{2}$H$_2$O),[20] respectively. The former two crystals have a bilayer structure with interdigitated alkyl chains (Type I), but the latter two crystals have a structure in which the terminal methyl groups formed have a plane facing each other instead of the interdigitation (Type F). The occupied area of an alkyl chain in the four crystals is 18.9, 17.7, 20.6 and 18.7 Å^2, respectively. The major difference between Type I and Type F structures is observed in the occupied area of the hydrophilic head which is larger in Type I than in Type F. The former and latter have larger occupied areas of the head group than the areas of one and two alkyl chains, respectively. The size of the head group is a crucial factor for determining the packing system of the alkyl chain between Type I and Type F. Crystals of MSAs have the Type I structure, because the bulkiness of the ester group increases the area of the head group. The alkyl chain in the crystals of most amphiphiles is inclined to the perpendicular of the *ab* plane by angles of 26, 11 and 45°, for DG, SDS·$\frac{1}{8}$H$_2$O and SDS·$\frac{1}{2}$H$_2$O, respectively. The decline contributes to the close packing of the alkyl chains. Because the occupied area of the hydrophilic head group is larger than that of the alkyl chain, the packing will be loose if the alkyl chain is packed perpendicularly. A characteristic of the amphiphile packing is expressed by eqn. (9),[31] where S is the occupied area

$$S \cos \varphi = n \times \Sigma \quad (9)$$

of the alkyl chain in the plane perpendicular to the chain axis, φ is the angle made by the alkyl chain and the normal to the bilayer, n is 1 for the Type F structure and 2 for the Type I structure, and Σ is the cross section of the alkyl chain. In the MSA crystals where the alkyl chain is slightly inclined, the occupied area of the head group is nearly twice that of the alkyl chain.

The result of the molecular mechanics calculations using the X-ray structure well describes the dependence of the thermal character of MSAs on the types of cations. The thermal stability of the crystals of MSA·K, **3** which is greater than that of MSA·Na, **1**, and MSA·Cs, **6** with the same length of alkyl chain, is related to the interaction between the anionic groups and the cations. The crystals of MSA·K salts have packing of

the potassium ions and sulfonato groups such that they obtain a crystal packing energy of electrostatic potential greater than that of MSA·Na and MSA·Cs. This tight packing of the potassium ion bundles anionic molecules against the repulsive interaction between sulfonato groups; therefore, the crystal packing energy is increased by the van der Waals force between the alkyl chains. The tight packing of the potassium salts reflects the atomic temperature factors of carbon atoms in the alkyl chain which are smaller than those of the sodium and cesium salts.

The water molecules of MSA·Na reduce the number of ionic contacts between the sodium ions and oxygen atoms of the sulfonato group in comparison with the MSA·K salts. The water molecules are bound to the cation and contribute to the decrease in the packing energy of the crystal. The enthalpy of the crystal of MSA·Na, which is a greater value than that of MSA·K and MSA·Cs salts, is ascribed to the hydration energy. The water molecule bound to the anionic molecules does not reduce the energy of the crystal packing as indicated by the molecular mechanics calculations because of the repulsion between the negatively charged oxygen atom of the water molecule and the sulfonato group in spite of the negative hydrogen bonding energy.

The alkyl chain moiety increases the thermal stability of the MSA·K crystal. The melting point is increased with the increase in the alkyl chain length. The van der Waals energy calculated using the Lennard-Jones potential in the molecular mechanics is also increased by the expansion of the alkyl chain. The thermal stability of some of the glycolipid crystals was not increased by the expansion of the alkyl chain.[11] The alkyl chains of MSA salts are packed closer than those of the glycolipid. The loose packings of the alkyl chain for the glycolipid do not cause a clearer increase of the melting points and enthalpies than MSA·K salts with tight packing of the chain.[11]

The calorimetric difference in the thermal stability between the crystals of MSA·Na and MSA·Cs is not consistent with the results of the molecular mechanics calculations. The statistical analysis of the molecular mechanics calculations did not explain the difference in the thermal stability between MSA·Na and MSA·Cs. The enthalpy of MSA·Na is smaller than that of MSA·Cs. The sodium salts have higher total crystal packing energy, E_{tot}, and greater interaction between the anionic molecule and cation than those of the cesium salts, in spite of the higher melting point of the crystal of MSA·Cs than MSA·Na.

Conclusions

The thermal stability of the crystals is affected by the packing of structural elements, especially by the interaction of the sulfonato group with the cation. Closely packed alkyl chains also contribute to the stability of the crystal structure, but the close packing causes a repulsive interaction between anionic groups which need to be stabilized by cations. The potassium salts form the most stabilized crystals of the three types of salts by the close packing of both the ionic components and the alkyl chain.

References

1 K. Noguchi, K. Okuyama and K. Vongbupnimit, *Mol. Cryst. Liq. Cryst.*, 1996, **276** 185.
2 S. Sundell, *Acta Chem. Scand.*, *Ser. A*, 1977, **31**, 799.
3 R. Pearson, H. Pearson and I. Pascher, *Nature*, 1979, **281**, 499.
4 R. G. Laughlin, *The Aqueous Phase Behaviour of Surfactants*, pp. 106–117, Academic Press, London, 1995.
5 A. J. Stirton, R. G. Bistline, Jr., A. B. Elizabeth and M. V. Nunéz-Ponzoa, *J. Am. Oil Chem. Soc.*, 1965, **42**, 1078.
6 N. M. Van Os, G. J. Danne and T. A. B. M. Bolsman, *J. Colloid Interface Sci.*, 1987, 115, 402.
7 M. J. Schick and J. M. Fowkes, *J. Phys. Chem.*, 1957, **61**, 1062.
8 E. D. Goddard, O. Harva and T. G. Jones, *Trans. Faraday Soc.*, 1953, **49**, 980.
9 F. F. Rawlings and E. C. Lingafelter, *J. Am. Chem. Soc.*, 1955, **77**, 870.
10 D. A. Lutz, J. K. Weil, A. J. Stirton and L. P. Witnauer, *J. Am. Oil Chem. Soc.*, 1961, **38**, 493.
11 Y. Abe, K. Harata, M. Fujiwara and K. Ohbu, *J. Chem. Soc.*, *Perkin Trans. 2*, 1998, **2**, 12.
12 Y. Abe, K. Harata, M. Fujiwara and K. Ohbu, *Carbohydr. Res.*, 1995, **269**, 43.
13 Y. Abe, K. Ohbu, M. Fujiwara and K. Harata, *Carbohydr. Res.*, 1995, **275**, 9.
14 Y. Abe, K. Harata, M. Fujiwara and K. Ohbu, *Langmuir*, 1996, **12**, 636.
15 P. C. Moews and J. R. Knox, *J Am. Chem. Soc.*, 1976, **98**, 6628.
16 G. A. Jeffrey, *Acc. Chem. Res.*, 1986, **19**, 168.
17 V. Zabel, A. Müller-Fahrnow, R. Hilgenfeld, W. Saenger, B. Pfannemüller, V. Enkelmann and W. Welte, *Chem. Phys. Lipids*, 1986, **39**, 313.
18 T. R. Lomer, *Acta Crystallogr.*, 1963, **16**, 984.
19 M. Goto and E. Asada, *Bull. Chem. Soc.*, *Jpn.*, 1978, **51**, 70.
20 V. M. Coiro, F. Mazza and G. Pochetti, *Acta Crystallogr.*, *Sect. C*, 1986, **42**, 991.
21 M. Fujiwara, M. Miyake and Y. Abe, *Colloid Polym. Sci.*, 1993, **271**, 780.
22 M. Fujiwara, Y. Kaneko and K. Ohbu, *Colloid Polym. Sci.*, 1995, **273**, 1055.
23 M. Fujiwara, T. Okano, T.-H. Nakashima, A. A. Nakamura and G. Sugihara *Colloid Polym. Sci.*, 1997, **275**, 474.
24 M. Fujiwara, T. Okano, H. Amano, H. Asano and K. Ohbu, *Langmuir*, 1997, **13**, 3345.
25 K. Ohbu, M. Fujiwara and Y. Abe, *Progr. Colloid Polym. Sci.*, 1998, **109**, 85.
26 G. Sheldrick, R. Herbst-Irmer and B. Clegg, SHELX WORKSHOP, Montreal, ACA, 23rd July 1995, pp. 1–29.
27 B. R. Brooks, R. E. Bruccoleri, B. D. Olason, D. J. States, S. Swaminathan and M. J. Karpuls, *J. Comp. Chem.*, 1983, **4**, 187.
28 R. Herbst, T. Steiner, B. Pfannemüller and W. Saenger, *Carbohydr. Res.*, 1995, **269**, 29.
29 V. Vand, *Acta Crystallogr.*, 1965, **19**, 798.
30 R. D. Shannon, *Acta Crystallogr.*, *Sect. A*, 1976, **32**, 751.
31 H. Hauser, I. Pascher, R. H. Pearson and S. Sundell, *Biochim. Biophys. Acta*, 1981, **650**, 21.

Paper 8/06314A